European Journal of Pharmaceutical Sciences 101 (2017) 22–30

Contents lists available at ScienceDirect

European Journal of Pharmaceutical Sciences

journal homepage: www.elsevier.com/locate/ejps

Preparation and characterisation of vandetanib-eluting radiopaque beads for locoregional treatment of hepatic malignancies

Alice Hagan [a,b,*], Gary J. Phillips [a], Wendy M. Macfarlane [a], Andrew W. Lloyd [a], Peter Czuczman [b], Andrew L. Lewis [b]

[a] School of Pharmacy and Biomolecular Sciences, University of Brighton, Moulsecoomb, Brighton BN2 4GJ, UK
[b] Biocompatibles UK Ltd., BTG International Group Company, Lakeview, Riverside Way, Watchmoor Park, Camberley GU15 3YL, UK

ARTICLE INFO

Article history:
Received 30 November 2016
Received in revised form 24 January 2017
Accepted 25 January 2017
Available online 27 January 2017

Keywords:
Vandetanib
Tyrosine kinase inhibitors
Drug-eluting beads
Transarterial chemoembolization

ABSTRACT

Since their introduction around a decade ago, embolic drug-eluting beads (DEBs) have become a well-established treatment option for the locoregional transarterial treatment of hepatic malignancies. Despite this success, the therapy is seen to be limited by the choice of drug and more effective options are therefore being sought. These include the small molecule multi-tyrosine kinase inhibitors (MTKi), which exert an anti-angiogenic and anti-proliferative effect that could be highly beneficial in combating some of the unwanted downstream consequences of embolization. Vandetanib is an MTKi which acts against such targets as vascular endothelial growth factor receptor (VEGFR) and epithelial growth factor receptor (EGFR) and has demonstrated modest activity against hepatocellular carcinoma (HCC), albeit with some dose-limiting cardiac toxicity. This makes this compound an interesting candidate for DEB-based locoregional delivery. In this study we describe the preparation and characterisation of vandetanib DEBs made from DC Bead™ and its radiopaque counterpart, DC Bead LUMI ™. Drug loading was shown to be dependent upon the pH of the drug loading solution, as vandetanib has multiple sites for protonation, with the bead platform also having a fundamental influence due to differences in binding capacities and bead shrinkage effects. Fourier transform infrared (FTIR) spectroscopy and energy dispersive X-ray (EDX) Spectroscopy confirmed drug interaction is by ionic interaction, and in the case of the radiopaque DEB, the drug is distributed uniformly inside the bead and contributes slightly to the overall radiopacity by virtue of a bromine atom on the vandetanib structure. Drug release from both bead platforms is controlled and sustained, with a slightly slower rate of release from the radiopaque bead due to its more hydrophobic nature. Vandetanib DEBs therefore have suitable characteristics for intra-arterial delivery and site-specific sustained release of drug into liver tumours.

1. Introduction

The current standard of care for intermediate hepatocellular carcinoma (HCC) is transarterial chemoembolization (TACE), an image guided procedure in which a chemotherapeutic agent is injected *via* the hepatic artery into the tumour feeding blood vessels. This is followed by an embolic material which occludes the vessels, with the aim of starving the tumour of oxygen and nutrients (Bruix et al., 2004). TACE may also be performed using drug eluting beads (DEB): embolic microspheres capable of loading positively charged drugs and releasing them local to the tumour site *via* ion exchange, thus reducing systemic drug exposure (Lewis and Holden, 2011). The drug of choice for loading into DEB is usually doxorubicin, a cytotoxic agent which intercalates with DNA, interfering with replication (Gewirtz, 1999). However, it has been shown that hypoxic conditions can lead to doxorubicin resistance in HCC cells (Cox and Weinman, 2015). Moreover, tumour hypoxia induced by embolization therapy leads to upregulation of pro-angiogenic pathways contributing to the formation of new blood vessels (Liang et al., 2010; Rhee et al., 2007). Anti-angiogenic strategies are therefore being considered in combination with DEBs to improve treatment outcomes.

Several trials combining TACE with oral anti-angiogenic therapy such as sorafenib, sunitinib or bevacizumab are underway or completed with some promising results, however there remain toxicity issues associated with oral use of these agents (Lencioni et al., 2016; Erhardt et al., 2014). DEBs provide an opportunity for local delivery of these agents, allowing for high local doses and reduced toxicity compared with oral treatment. Forster et al. were the first to demonstrate that DEBs could be loaded with a combination of drugs (Forster et al.,

Abbreviations: MTKi, multi-tyrosine kinase inhibitor; RODEB, radiopaque drug-eluting bead; HCC, hepatocellular carcinoma.

* Corresponding author at: School of Pharmacy and Biomolecular Sciences, University of Brighton, Moulsecoomb, Brighton BN2 4GJ, UK.
E-mail address: alice.hagan@btgplc.com (A. Hagan).

http://dx.doi.org/10.1016/j.ejps.2017.01.033

2012), not only to provide the benefit of local delivery of a cytotoxic drug such as doxorubicin, but also concomitant delivery of an agent with a complimentary mode of action such as rapamycin in order to downregulate expression of Hypoxia Inducible Factor Alpha (HIF-1α) and consequently induction of angiogenesis. Sakr et al. have more recently described a layer-by-layer process for loading bevacizumab onto DC Bead™ (Sakr et al., 2016) for controlled locoregional delivery of a monoclonal antibody that inhibits Vascular Endothelial Growth Factor-A (VEGF-A), a chemical signal for angiogenesis. It is however, the small molecule multi-tyrosine kinase inhibitors that have attracted most interest, given the approval of sorafenib (Nexavar®, Bayer-Onyx) for the treatment of advanced HCC. Sorafenib drug-eluting peptide nanocomposites (Park et al., 2016) and poly(lactide-*co*-glycolide) microspheres (Chen et al., 2014; Chen et al., 2015), both with magnetic resonance imaging (MRI) capability have been described for intra-arterial delivery to treat HCC. Poly(D,L-lactic acid) microspheres have also been prepared and loaded with either sorafenib or together with cisplatin and showed that the drug combination had a faster release rate (Wang et al., 2015) and was more efficacious in cell assays (Wang et al., 2016) compared to either drug alone. Lahti et al. described the loading of LC Bead with both sorafenib (Lahti et al., 2015a) and sunitinib (Lahti et al., 2015b) but both processes were inefficient. Fuchs et al. have reported on a much more comprehensive appraisal of sunitinib loading into DC Bead™ (Fuchs et al., 2015), correlation of *in vitro* release with *in vivo* pharmacokinetics (Fuchs et al., 2014) and evaluation of antitumor effects in a rabbit VX2 embolization model (Bize et al., 2016). Whilst these studies show great promise and demonstrate feasibility for the locoregional delivery of MTKis from DEBs, concerns remain over the severe toxicity of sunitinib in the liver (Cheng et al., 2013) and alternative suitable MTKi candidates have been sought.

Table 1 outlines a short selection from a broad list of options that have been considered for MTKi loading into DEBs, taking into account drug structure, properties and mode of action. Herein we describe a feasibility study undertaken with one of these candidates, vandetanib. Vandetanib is a multi-tyrosine kinase inhibitor (MTKi) which selectively inhibits vascular endothelial growth factor receptor 2 (VEGFR-2), epidermal growth factor receptor (EGFR), and rearranged during transfection (RET) tyrosine kinase (Morabito et al., 2009). Common adverse events associated with the oral delivery of vandetanib include diarrhoea and rash, which can occasionally be severe. Prolongation of the QT interval (a measure of the time between the start of the Q wave and the end of the T wave in the heart's electrical cycle and a marker for the potential of ventricular tachyarrhythmias) has also been observed (Tsang et al., 2016). The VEGF and EGF pathways have both been implicated in the pathogenesis of HCC, and a phase II trial of vandetanib in advanced unresectable HCC patients showed a suggestion of improvement in progression free survival and overall survival (Hsu et al., 2012). There is therefore, a strong rationale for the locoregional delivery of this drug.

In this study the feasibility of loading vandetanib into DEB was investigated using both DC Bead™ and the recently approved radiopaque DEB DC Bead LUMI™ (Biocompatibles UK Ltd., Farnham, UK). This has resulted in an understanding of the interactions between vandetanib and the hydrogel network of the microspheres and the physicochemical characteristics of the resulting vandetanib-eluting beads in terms of maximum drug loading capacity, morphology, drug distribution and release.

2. Materials and methods

2.1. Materials

DC Bead™ and DC Bead LUMI™, both of diameter range 70–150 μm, were provided by Biocompatibles Ltd. (Farnham, UK). Vandetanib base was provided by Astra Zeneca (Macclesfield, UK, >99% purity).

Table 1
Selection of MTKis and their mode of action and properties.

Compound	Mode of action	Properties[a]
Axitinib	Potent VEGF inhibitor, inhibits breast cancer growth, prevents neoangiogenesis in 9 L tumours, activity in refractory met renal cell	DMSO + DMF soluble Solubility of over 0.2 μg/mL in aq media with a pH 1.1–7.8, pKa 4.8
Bosutinib	Active inhibitor of Bcr-Abl, inhibits tumour cell growth, angiogenesis, growth factor expression	DMSO + EtOH soluble, poorly water soluble Basic pKas 8.04, 4.80, 3.77
Canertinib diHCl	Potent pan-erb B tyrosine kinase inhibitor, irreversible TK inhibitor, radiosensitiser	10 mg/mL water solubility, DMSO ≥5.6 mg/mL, logPc 3.05
Dasatinib	SRC and BCR/ABL tyrosine kinase inhibitor, Lyn & Src kinase inhibitor	Very poorly water soluble (0.0128 mg/mL), pKas 3.1, 6.8, logP 1.8
Dovitinib	MTKi of FGFR 3, inhibits tumour growth in xenograft models of colon cancer	DMSO soluble, poorly EtOH soluble
Erlotinib HCl	Targets EGFRTK, potent inhibitor of JAK2-V617F. "Tarcecva" approved for NSCLC, pancreatic and others	Slight water and methanol solubility, pKa 5.42, logP 2.7
Gefitinib	EGFR TK inhibitor. "Iressa" approved for NSCLC	Solubility 0.027 mg/mL, sparingly water soluble at pH 3, pKas 5.4, 7.2, logP 3.2
Imatinib methane-sulfonate	Inhibits particular TK enzymes, used to decrease bcr-abl TK activity. Gleevec®, indicated for chronic myelogenous leukemia, GI stromal tumours	DMSO and water soluble, poorly EtOH soluble, logP 3
Lapatinib toluene-sulfonate	EGFR and HER2/neu dual TK inhibitor, potent EGFR kinase inhibitor, can restore tamoxifen sensitivity. "Tykerb®" for advanced met breast cancer	Poorly water soluble (0.0223 mg/mL), DMSO soluble, logP 5.4
Lestaurtinib	Potent inhibitor of several TKs FLT-3, TrkA, clinical activity in AML pts. with FLT-3 mutations	Very poorly water soluble
Masitinib	Protein TK inhibitor, phase III in dogs with canine mast cell tumours	Soluble in DMSO ≥95 mg/mL, water <1.2 mg/mL
Nilotinib	Selective BCR-ABL inhibitor and of proliferation of haematopoietic cells in CML and ALL. TK inhibitor Ph I in CML "Tasigna®"	Poorly water (0.00201 mg/mL) and poorly EtOH soluble, DMSO soluble, logPc 4.51
Pazopanib	Selective multitargeted TK inhibitor, targets VEGFR, PDGFR and c-kit	Limited solubility in warm DMSO, poorly water soluble (0.0433 mg/mL) logPc 3.59
Sorafenib toluene-sulfonate	Biaryl urea inhibits ERK pathway and angiogenesis by targeting VERGFR-2 and PDGRF-b. "Nexavar®" approved renal cell carcinoma and HCC	Poorly water (0.00171 mg/mL) and EtOH soluble, DMSO soluble, logP 3.8
Sunitinib Malate	Selective inhibitors of MTKs, inhibits FLT3-ITD phosphorylation, CSF-1 rK. "Sutent®" for renal cell carcinoma	Water soluble at pH 1.2–6.8, fluorescent, weak base pKa 8.95, logP 5.2
Vandetanib	VEGFR-dependent tumour angiogenesis inhibitor, EGFR & RET-dependent proliferation inhibitor. "Zactima®" for follicular, medullary, anaplastic, adv/met papillary thyroid cancer	DMSO soluble, poorly water soluble (0.008 mg/mL), soluble at lower pHs, logPc 5.01
Vatalanib DiHCl	Selective inhibitor for	Water soluble (10 mg/mL),

Table 1 (*continued*)

Compound	Mode of action	Properties[a]
	VEGFR-1&2 TK + PDGFR-b, c-KIT & c-FMS	DMSO soluble (85 mg/mL)

[a] Information sourced from www.drugbank.ca or individual drug FDA labels.

2.2. Loading of beads with vandetanib solution

As vandetanib exhibits pH dependent solubility, solutions were prepared by first dissolving the powdered drug in 0.1 M hydrochloric acid to 70% of the required volume. The solution was then adjusted to the required pH by dropwise addition of sodium hydroxide, before making up to volume with purified water. By this protocol, solutions at pH 2.1 and 4.4 were prepared at a concentration of 20 mg/mL. Solutions at pH 6.8 were prepared at a concentration of 5 mg/mL due to limits in solubility.

To load beads with vandetanib, the packing solution was removed from bead vials and vandetanib solution was added. Incubation with the loading solution was performed at room temperature under agitation for a minimum of 2 h. Depleted loading solution was removed and the beads washed 3 times in deionised water. To determine loading efficiency, vandetanib concentration in the depleted loading solution and washings was quantified by HPLC, using a Hypersil Gold C18 column (Thermo Scientific, UK) and PDA detector at a wavelength of 254 nm. Mobile phase was a gradient of 0.1% TFA v/v in purified water and 0.1% TFA v/v in methanol; flow rate 1 mL/min.

2.3. Bead morphometry

Bead samples before and after vandetanib loading were examined using an Olympus BX50 optical microscope with attached Colorview III camera. The diameter of 200 beads per sample was recorded using Stream software (Olympus, Southend on Sea, UK). Bead density was determined using a displacement assay described in detail previously (Duran et al., 2016).

2.4. Elemental mapping using SEM-EDX

DC Bead LUMI™ was loaded with the maximum vandetanib dose of 135 mg/mL of sedimented beads. Bead samples were embedded in Tissue-Tek optimum cutting temperature compound (Sakura, Thatcham, UK) on liquid nitrogen and transferred to −80 °C to ensure thorough freezing. Samples were sectioned in a cryostat (Leica, Milton Keynes, UK) in 10 μm thick sections and mounted on SEM stubs with carbon pads. Samples were coated with 4 nm platinum using a Q150T turbo molecular-pumped sputter coating system (Quorum, Lewes, UK) prior to SEM-EDX analysis. SEM imaging was carried out on a Zeiss SIGMA FEG-SEM (Zeiss, Cambridge, UK) scanning electron microscope equipped with an Oxford Instruments 80 mm^2 X-Max energy dispersive X-ray analysis system. The sample was left in the SEM for several minutes prior to imaging to ensure the small amount of water present in the section was removed under the high vacuum. Elemental mapping and spectra were acquired for iodine, bromine, fluorine and sulfur on unloaded DC Bead LUMI™ and DC Bead LUMI™ loaded with vandetanib at maximum capacity.

2.5. Vandetanib-bead interactions using Fourier transform infra-red microscopy

DC Bead LUMI™ loaded with different doses of vandetanib were embedded and sectioned into 10 μm slices as described in Section 2.4. These were subjected to FTIR microscopy point analysis across a 10–15 different regions of interest across the samples surface. The spectra were collated and the position of the S═O stretching frequency around 1040–1050 cm^{-1} was averaged for each sample. The effect of differing concentrations of drug loading on the stretching absorption of the sulfonate binding groups on the beads could then be evaluated.

2.6. X-ray micro-computer tomography (μ-CT) analysis for bead radiopacity

Unloaded LUMI™ and LUMI™ loaded with vandetanib at concentrations of 30, 60 and 100 mg/mL were uniformly suspended in 1% agarose solution in nunc tubes. μ-CT 3D scanning was performed to quantify individual bead radiopacity in Hounsfield units (HU) of each bead in the sample. μ-CT analysis was performed by Reading Scientific Services Ltd., Reading, UK.

2.7. Vandetanib release from beads

DC Bead™ and DC Bead LUMI™ were loaded with 20 mg/mL and 40 mg/mL of vandetanib respectively. The volume of DC Bead™ decreased by 50% following loading leading to a final dose density of 40 mg/mL. Aliquots of 0.3 mL of beads each containing 12 mg vandetanib were placed in amber jars containing 1 L of pH 7 PBS (Source Bioscience, Nottingham, UK), stirring at 200 rpm. At determined time points, stirring was stopped to allow beads to settle before removing a 5 mL sample of PBS for vandetanib quantification by HPLC as described in Section 2.2. 5 mL of fresh PBS was replaced after each timepoint.

2.8. Evaluation of suspension, handling and administration of vandetanib loaded DC Bead LUMI™

A series of evaluations were conducted to ensure that loading of vandetanib into the beads did not adversely affect their handling and delivery through a microcatheter. DC Bead LUMI™ (70–150 μm) was loaded with 100 mg/mL of vandetanib as described in Section 2.2, excess loading solution removed and the bead slurry (1 mL) mixed with contrast agent (9 mL Omnipaque 350®, GE Heathcare, Oslo, Norway). After transferring into a 20 mL Luer-lok™ syringe (BD Plastipak, Temse, Belgium) a three-way stopcock (Discofix®, B. Braun, Melsungen, Germany) was attached to the syringe and another syringe attached to enable transfer between them for suspension. Beads were transferred between two syringes in injection mixture of Omnipaque 350® and water 20 times. Suspension time was measured by the time it took for 25% of the solution to be free from beads, *i.e.* time taken for the top of the bead suspension to fall to 75% of the internal height of the syringe ($n = 3$). The suspension was passed through a 2.4 Fr catheter (Progreat®, Terumo Corp., Tokyo, Japan) and the beads assessed visually for any signs of deformation of their shape or presence of fragmentation using optical microscopy as in Section 2.3.

2.9. Stability of vandetanib loaded DC Bead LUMI™ contrast agent suspension

When used in hospital, on occasion DEBs are often prepared in the hospital pharmacy the night before and stored in a refrigerator. Drug elution from vandetanib loaded DC Bead LUMI™ (70–150 μm) suspended in contrast agent was therefore investigated by taking aliquots of the delivery media supernatant over a period of 24 h and analysing them using the HPLC method described in Section 2.2 to determine the amount of vandetanib eluted ($n = 3$). The chromatographic peak was also analysed to determine if there was any drug degradation during this period.

3. Results

3.1. Vandetanib loading and maximum capacity

At acidic pH, positively charged amines on vandetanib molecules interact with negatively charged sulfonate groups within the microsphere

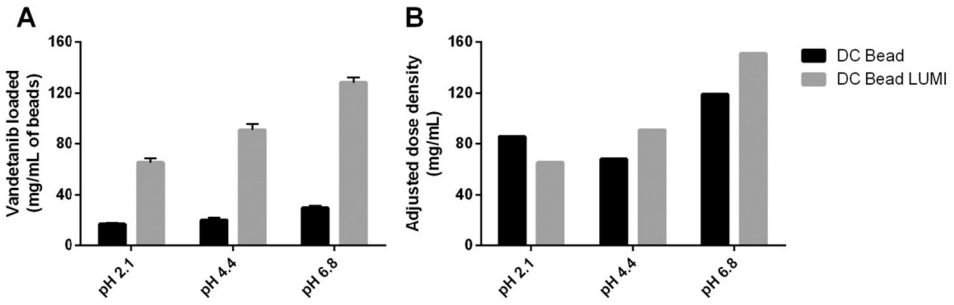

Fig. 1. Maximum loading of vandetanib in DC Bead™ and DC Bead LUMI™ at varying pH. A) Amount of drug uptake per mL of beads (initial volume), bars represent mean ± SD, n = 5; B) dose density per mL of beads after adjustment for loading induced bead shrinkage.

hydrogel network, enabling drug loading. From the theoretical prediction shown in Fig. 8, the major vandetanib microspecies, a 2+ charged form and a 1+ charged form, are predominant at pH 2.1 and pH 6.8 respectively, with a 50:50 proportion of each form at pH 4.4. Vandetanib solutions were prepared at each of these pHs and added to beads in excess to assess the effect on maximum loading capacity.

Maximum vandetanib capacity increased with pH (proportion of 1+ form) as expected, with maximum capacity at 30 mg/mL for DC Bead™ and 135 mg/mL for DC Bead LUMI™ (Fig. 1). Initial analysis of depleted loading solution from DC Bead™ showed a higher than expected loading efficiency, but with subsequent washes in water the actual loading dose was found to be lower suggesting that some drug was weakly associated with the bead surface and able to be removed with water. This effect was less pronounced with DC Bead LUMI™. Below maximum capacity, a loading efficiency of >99% was achieved after 2 h of incubation with loading solution, suggesting fast adsorption of vandetanib into beads. When considering the respective chemical compositions of both beads, the theoretical maximum loading capacity based upon the content of sulfonic acid drug binding residues is higher for both DC Bead™ and DC Bead LUMI™ than the actual experimentally determined maximum drug binding capacity. For DC Bead, the maximum amount of drug loaded varies from 81 to 91.2% of the theoretical, compared to 74.5–80.4% for DC Bead LUMI™, both dependent upon the pH of the loading solution.

3.2. Bead morphology, size and density after loading

After loading with vandetanib, beads retained a smooth, spherical appearance (Fig. 2A–D). Loading DC Bead M1™ at maximum vandetanib capacity caused a significant decrease in mean diameter (35%, $p < 0.0001$) as well as a narrowing of the size distribution (Fig. 2E). The size decrease showed a trend with decreasing pH. The size reduction corresponded with a reduction in settled bead volume of over 60%. The bead density increase from 1.03 ± 0.03 g/cm^3 (unloaded) to 1.15 ± 0.09 g/cm^3 (loaded at 30 mg/mL), this small increase due to the decrease in size and contraction of the matrix. In contrast, the mean diameter of DC Bead LUMI™ loaded at maximum capacity did not significantly decrease at any pH (Fig. 2F), despite a 15% reduction in the settled bead volume at pH 6.8 only. The density increased only minimally from 1.29 ± 0.03 g/cm^3 (unloaded) to 1.31 ± 0.09 g/cm^3 when loaded at 100 mg/mL due to the marginal size change.

3.3. Vandetanib distribution in beads

Scanning electron microscopy showed the sectioned internal structure of DC Bead LUMI™ to be homogeneous and devoid of any visible pores (Fig. 3(a)). SEM-EDX analysis was used to detect vandetanib distribution in sectioned sample loaded at maximum capacity of 135 mg/mL. Bromine was selected as the element of interest for the

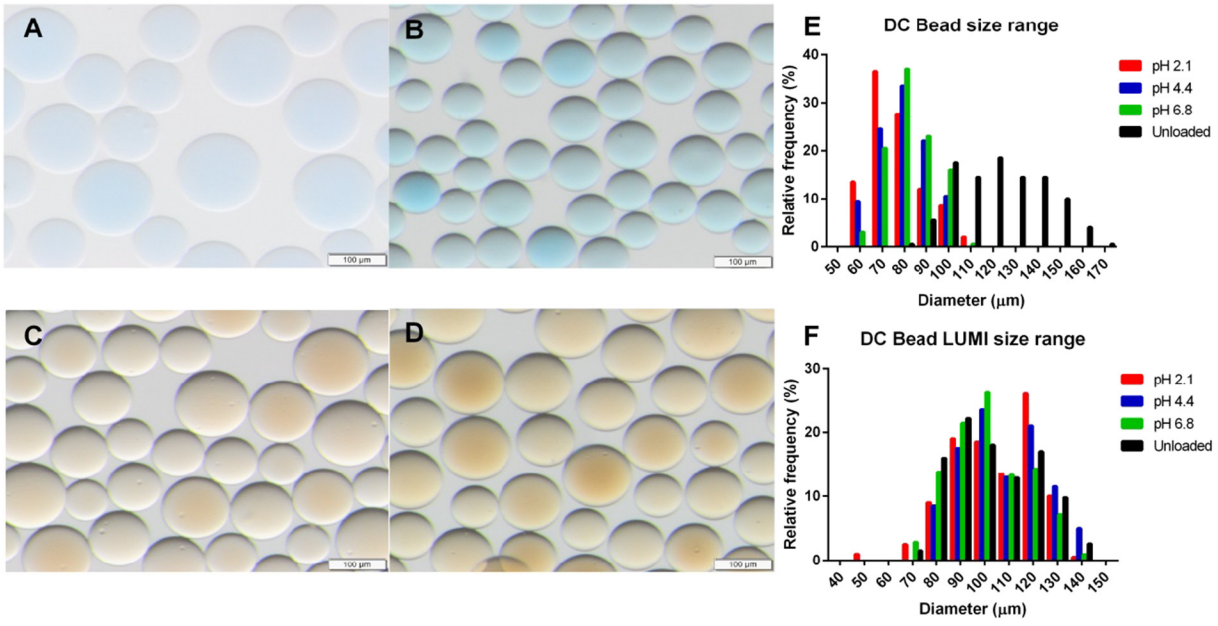

Fig. 2. (A) Unloaded DC Bead™; (B) vandetanib-loaded DC Bead™ (30 mg/mL, pH 4.6); (C) unloaded DC Bead LUMI™; (D) vandetanib-loaded DC Bead LUMI™ (100 mg/mL, pH 4.6). Scale bars 100 µm. (E) DC Bead™ and (F) DC Bead LUMI™ size decrease after vandetanib loading at differing pHs.

drug distribution, being present in vandetanib molecules but not in DC Bead LUMI™. The sulfur and iodine distributions were also mapped to gain insight into the bead internal structure. Elemental mapping revealed that bromine was evenly distributed throughout the sectioned beads (Fig. 3(b)), the bromine peak seen in the EDX spectrum (arrow, Fig. 3(e)) being absent in the spectrum for control (unloaded) beads (data not shown). Sulfur and iodine distributions also appeared to be evenly distributed within the bead structure (Fig. 3(c) and (d)) (Duran et al., 2016). The table insert in Fig. 3(e) shows there is an excellent agreement between the measured weight percent of elements by EDX compared with the theoretical calculated weight percentage expected based upon 135 mg/mL loading of vandetanib into DC Bead LUMI™, the latter which possesses 177 mg/mL iodine (Duran et al., 2016).

3.4. Evaluation of drug-bead interactions using FTIR microscopy

As the dose of vandetanib loaded into DC Bead LUMI™ was increased, the frequency of the S ═O stretch from the sulfonate groups of the beads was seen to shift steadily to lower wavenumber (Fig. 4).

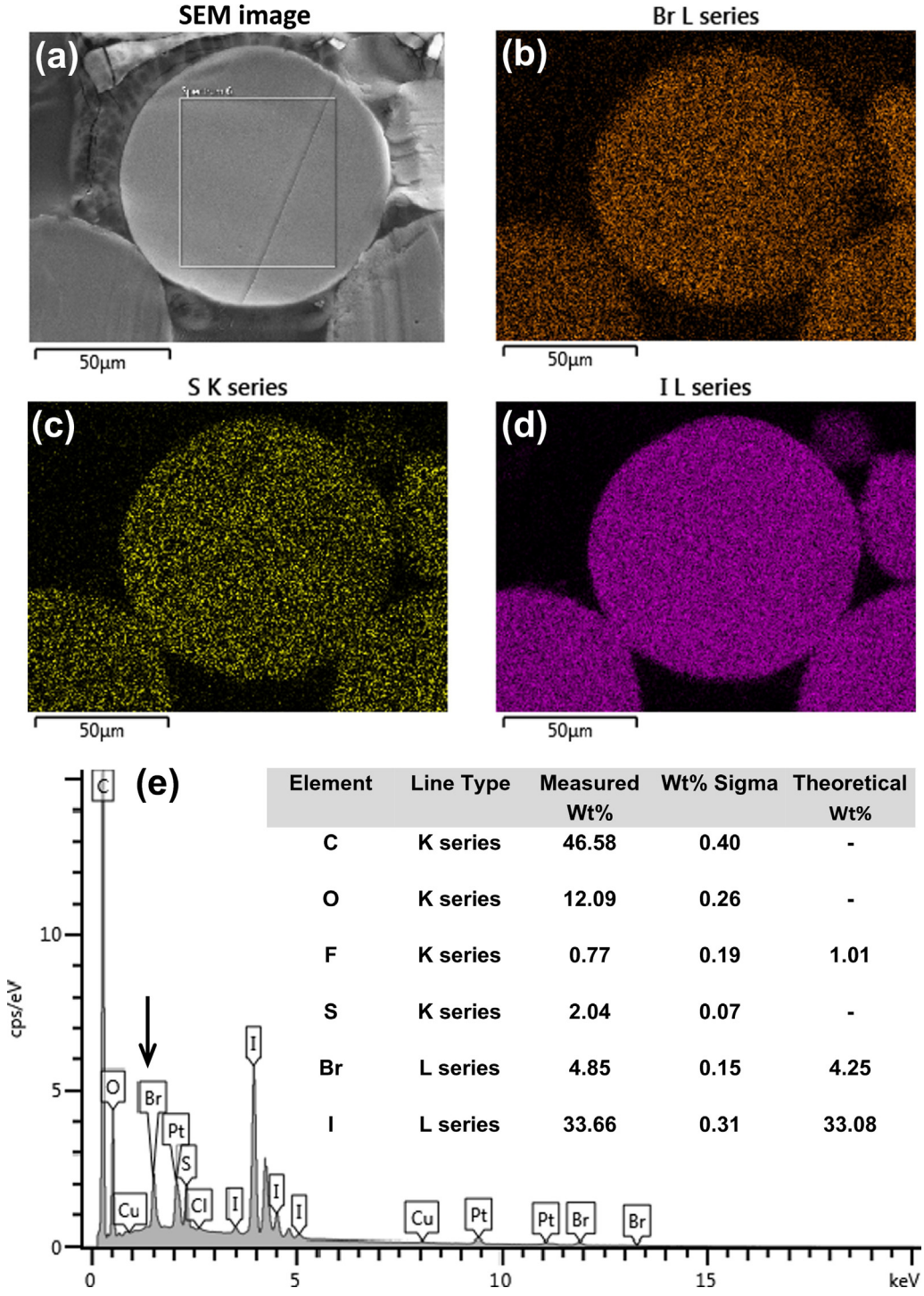

Element	Line Type	Measured Wt%	Wt% Sigma	Theoretical Wt%
C	K series	46.58	0.40	-
O	K series	12.09	0.26	-
F	K series	0.77	0.19	1.01
S	K series	2.04	0.07	-
Br	L series	4.85	0.15	4.25
I	L series	33.66	0.31	33.08

Fig. 3. (a) Scanning electron microscopy image of a sectioned vandetanib-loaded DC Bead LUMI™ sample; (b) bromine elemental mapping distribution image; (c) sulfur elemental mapping distribution image; (d) iodine elemental mapping distribution image; (e) EDX elemental spectrum showing bromine peak for the vandetanib loaded bead and elemental analysis (table inset).

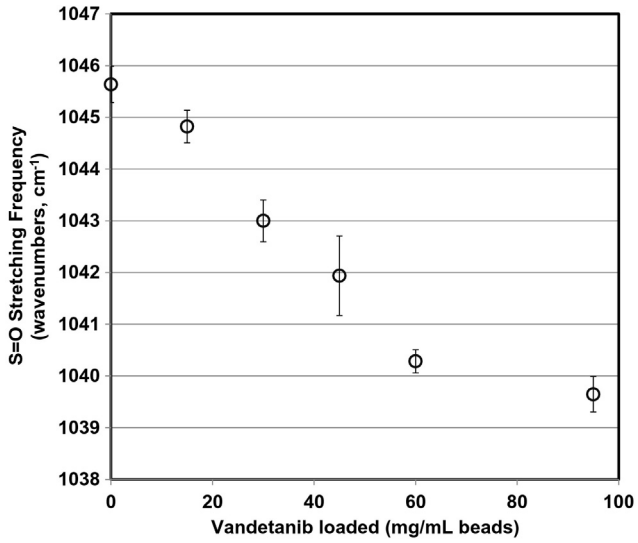

Fig. 4. Effect of vandetanib loading dose on the S ═O stretching frequency from the sulfonate groups on the beads (error bars = SEM).

This is indicative of an increasing interaction between drug and bead as all of the bead binding sites become progressively occupied. Samples loaded using a target loading of 60 mg/mL at pH 6.8, 4.4 and 2.1 gave rise to similar S ═O stretching frequencies at 1041.6 cm^{-1}, 1040.3 cm^{-1} and 1040.4 cm^{-1} respectively.

3.5. Radiopacity of vandetanib loaded DC Bead LUMI™

Micro-CT analysis of DC Bead LUMI™ shows it to possess an inherent radiopacity due to the triiodobenzyl moieties attached to the bead structure (Duran et al., 2016; Levy et al., 2016; Sharma et al., 2016), giving rise to a baseline radiopacity of 4454 ± 225 Hounsfield units. The level of radiopacity is seen to increase linearly with increasing loading of vandetanib into the beads (Fig. 5) until at a loading of 100 mg/mL of vandetanib, the radiopacity is seen to have increased by 621 Hounsfield Units.

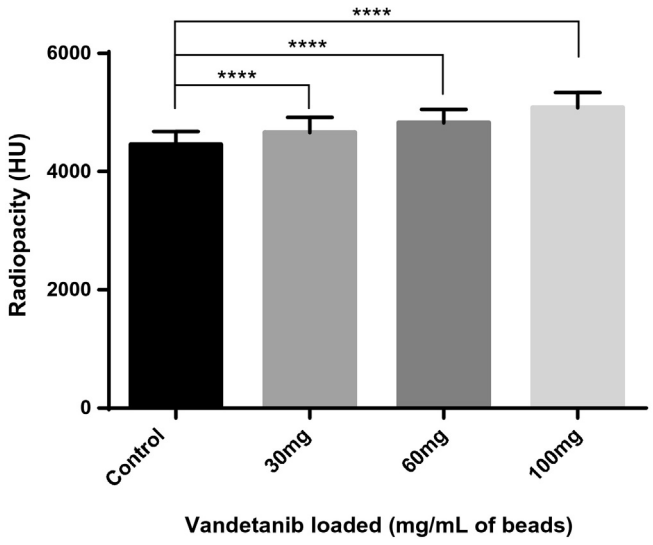

Fig. 5. Effect of vandetanib loading into DC Bead LUMI™ on radiopacity of the beads. Bars represent mean of all beads in a single scan of the sample (>6000 beads per sample) ± SD. **** = $p < 0.0001$ by 1 way ANOVA + Holm-Sidak's multiple comparisons test between doses.

3.6. Vandetanib release from beads

The elution of vandetanib from DC Bead™ and DC Bead LUMI™ into PBS was analysed using an *in vitro* USP type II dissolution model, using 0.3 mL aliquots of beads that had been loaded at equivalent dose densities of 40 mg/mL at pH 4.4 (12 mg per aliquot). Drug release showed a rapid burst phase in the first 2 h, after which it began to plateau (Fig. 6). The total percentage release of vandetanib over the test period was higher from DC Bead™ than from DC Bead LUMI™, achieving on average 85% drug release in 24 h, compared to an average of 50% from DC Bead LUMI™.

3.7. Evaluation of suspension, handling, delivery and stability of vandetanib loaded DC Bead LUMI™

When DC Bead LUMI loaded with 100 mg of vandetanib was suspended in Omnipaque 350® (Section 2.8) the beads formed a uniform suspension and showed no signs of bead agglomeration. The bead suspension did not adhere onto the surface of the vial and was easily transferred into a syringe for delivery. The average time in suspension within the syringe was >6.5 min which is more than sufficient for practical usage. The bead suspension was delivered through a 2.4 Fr microcatheter with ease and there was no occurrence of catheter blockage during bead delivery. The beads remained spherical with no signs of fragmentation post-delivery.

The amount of vandetanib released from the beads into the contrast medium 15 min after mixing was 3.3 mg, which increased to just 3.5 mg in total after 24 h storage. The drug was seen to be unaltered and remained within specification, >98.0% purity with no single impurity >0.2%. This shows that a bead suspension could be potentially prepared in advance and stored overnight without significant elution of drug into the delivery medium and without risk of drug degradation.

4. Discussion

Drug candidates that have been loaded into DC Bead™ have conventionally been water soluble cationic salt forms that allow for diffusion and ion-exchange into the anionically-charged hydrogel matrix of the bead (Forster et al., 2010; Guiu et al., 2015; Lewis, 2009; Lewis et al., 2007; Taylor et al., 2007). MTKis represent a group of small molecules with widely differing structures that impact drug solubility, lipophilicity and ionization potential. Different process strategies may therefore be required when considering how to load sufficient amounts of these compounds in an efficient way into the bead matrix, and subsequently what intermolecular drug-bead interactions will control the release of the molecule.

The chemical structures of a selection of MTKis considered for combining with DEBs are presented in Fig. 7. Sorafenib loading into DC Bead ™ has been reported but the low solubility of the drug in aqueous media requires a loading process of several sequential sessions of loading from low drug concentration solution to achieve sufficient quantities of loaded drug (Lahti et al., 2015a). This can be overcome by use of a DMSO swelling process in which drug dissolved in DMSO can be used to swell the beads, followed by a precipitation step as the drug swollen beads are immersed in water (Forster et al., 2012). This however, leaves the drug in a microprecipitated form in which its elution is dependent upon the dissolution of the particulates. The partial ethanol solubility of sorafenib can be used to produce suitable loading solutions in ethanol:water mixtures in which the drug can be exchanged into the bead matrix. Sorafenib however, unlike, many of the other MTKis, has no protonatable amine group and relies upon strong hydrogen bonding of the amines on the urea group to interact with carboxylate residues in at its target site. This may also provide a source of interaction between drug and bead to ensure controlled release.

Sunitinib on the other hand has a pendant tertiary diethyl substituted amine that can be protonated to provide a ionic interaction with the

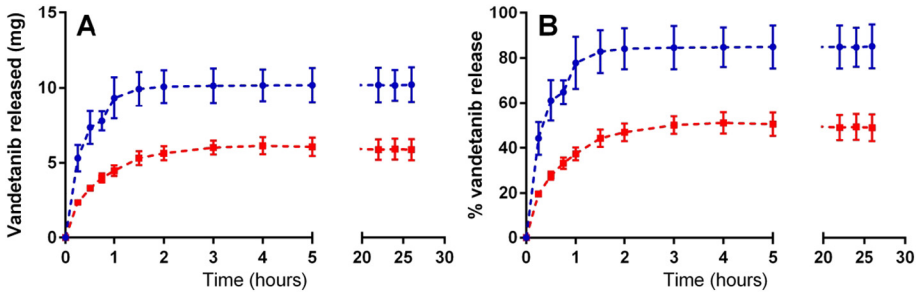

Fig. 6. Vandetanib release from DC Bead™ [●] and DC Bead LUMI™ [■] as A) amount released in mg; B) percentage of available dose. 0.3 mL aliquots of beads containing equivalent of 12 mg vandetanib were stirred in 1 L PBS, pH 7. Mean ± SD, n = 3.

beads (Lahti et al., 2015b.). Solubility is improved below pH 6.8 and is further enhanced with the addition of a sugar or polyol additive to aid loading (Fuchs et al., 2015). Vandetanib, erlotinib, gefitinib and dasatinib all share a common secondary amine bridging function attached to a pyrimidine ring, providing additional sites of ionization to aid in ion-exchange and increase the solubility of these compounds in water at reduced pH. The positive charge residing on this aromatic portion of the molecule however, can be significantly delocalised across the conjugated ring system, which lessens its capability for charge-charge interaction (Lewis, 2009).

Based on the theoretical ionization of vandetanib in solution at different pH (Fig. 8) and therefore the relative concentrations of different vandetanib charge forms, the drug loading maximum capacity should be influenced by the pH of the loading solution, which has been confirmed in Fig. 1. For both DC Bead™ and DC Bead LUMI™, there was a positive relationship between pH of the loading solution and the maximum amount of vandetanib that could be loaded into the beads. This is due to the fact that as pH decreases, a greater proportion of vandetanib molecules in solution have 2 positive charges, and can therefore occupy 2 sulfonate binding sites within the beads, shifting towards a 2:1 binding ratio. Regardless of the pH, neither bead was able to load the theoretical maximum drug loading based upon sulfonic acid group content, although DC Bead™ was seen to load closer to the theoretical maximum (91.2%) than DC Bead LUMI™ (80.4%), the latter having a denser, more hydrophobic gel matrix in which access to all binding sites may be more restricted.

In DC Bead™, a slight decrease in size range was observed with decreasing pH. This is in keeping with previously observed effects of loading the antineoplastic mitoxantrone, which has 2 positively charged sites, and thus exerts an increased shrinking effect on DC Bead™ which is suggested to be an effect of 'pulling' the hydrogel network closer together by interacting with multiple sites (Lewis, 2009). The drug-bead charge-charge interaction through the sulfonate groups was confirmed by the shift of the S ═O stretching frequency to lower wavenumber with increasing drug dose, a phenomenon also observed for both doxorubicin and irinotecan binding to DC Bead™ (Lewis and Dreher, 2012; Namur, 2009). Interestingly, when 60 mg/mL loading was performed at pH 2.1, 4.4 and 6.8, the S ═O frequency was seen not to change significantly, even though at this dose the DC Bead LUMI™ is only at about 50% binding capacity. At pH 2.1 it is expected that vandetanib would carry two positive charges and hence capable of interaction with nearly all binding sites in the beads. The second charge residing on the conjugated ring system would not be expected to interact as strongly as that on the piperidine ring as indicated by the lack of change in the S ═O stretching frequency.

Furthermore, although it could be expected that vandetanib molecules binding to 2 sites may be released more slowly in an elution model, the release profile of vandetanib from DC Bead LUMI™ did not vary significantly depending on the pH of the loading solution (data not shown). Possible reasons for this are that the ionic interactions are not strong enough to be affected in this manner, or perhaps the neutral pH of the elution medium negates this pH dependent effect as soon as the ion exchange process begins.

Release of vandetanib from DC Bead LUMI™ was incomplete, despite maximum concentrations reached in the elution vessel remaining lower than the theoretical solubility of 0.008 mg/mL (Fig. 6A). The higher

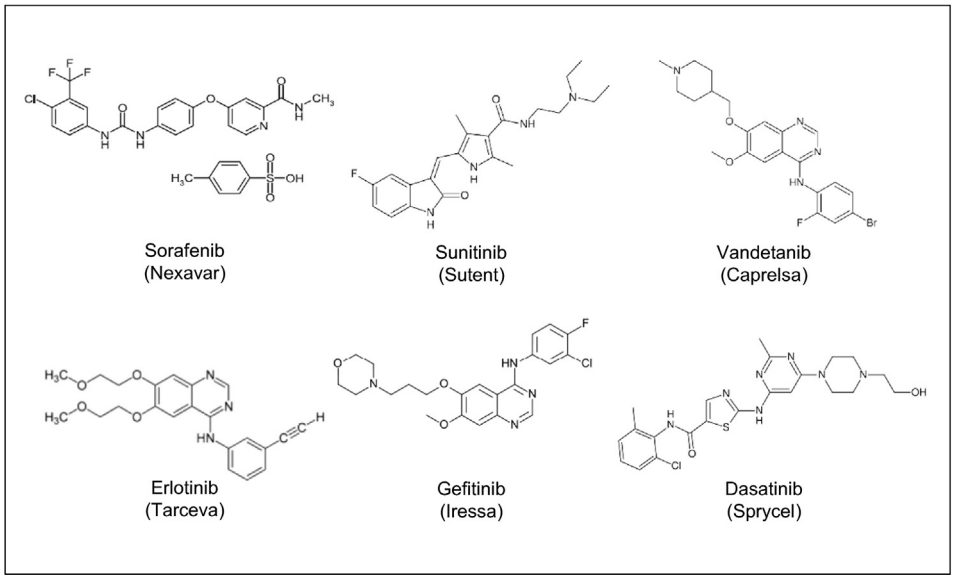

Fig. 7. Structure of a selection of approved MTKis.

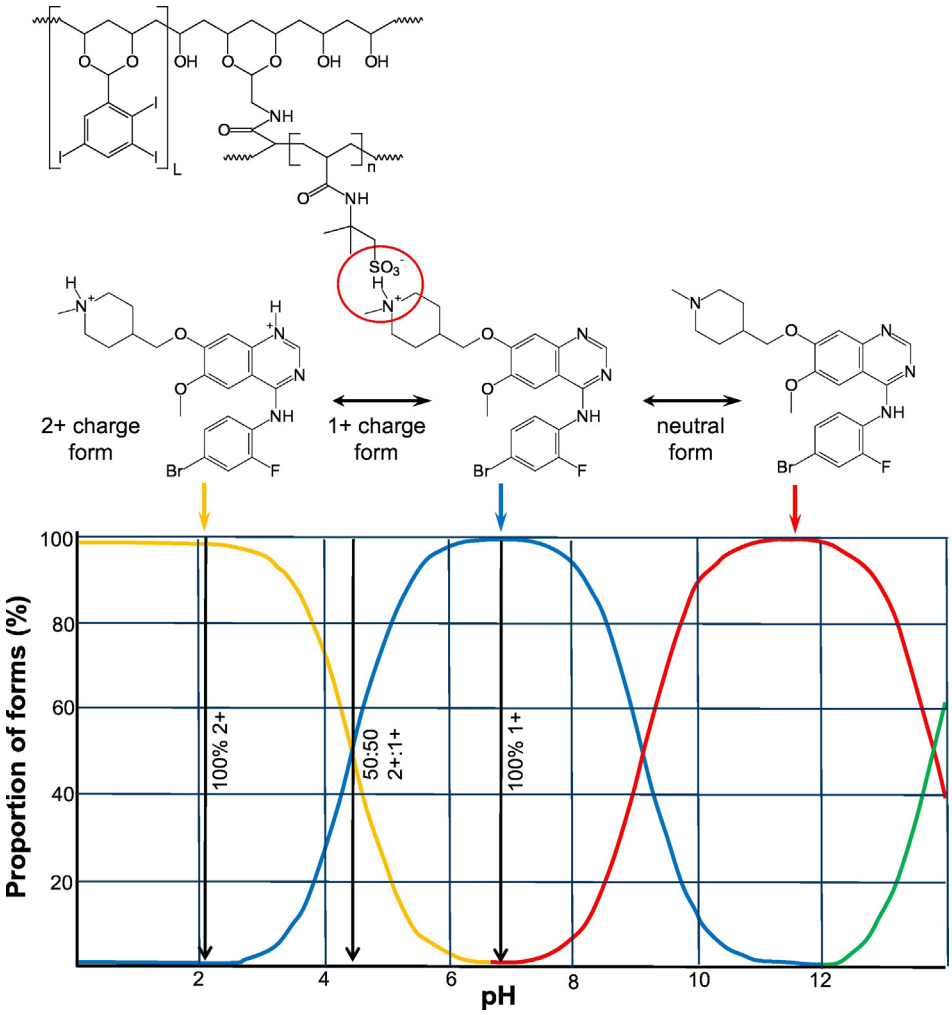

Fig. 8. Ionic interaction of DC Bead™ (L groups are present in DC Bead LUMI™) with vandetanib (top); structure of the ionised forms of vandetanib at different pH (middle); (c) theoretical proportion of the various forms of vandetanib present with pH (adapted from chemicalize.org).

density and therefore less 'open' structure of DC Bead LUMI™ likely limits movement of drug molecules out of the beads. However, by adjusting the pH of the PBS elution medium to 5, vandetanib release rate from LUMI™ was slightly improved with total drug release increasing by 10% to 60% (data not shown). Hypoxic tumours are known to be acidotic due to production of lactic acid by anaerobic glycolysis. Moreover efficient arterial embolization will impede clearance of lactic acid from tumoural tissues, contributing to the acidic microenvironment (Chao et al., 2016), which may somewhat facilitate release in the case of acidic-soluble drugs. Similarly to doxorubicin (Hecq et al., 2013), vandetanib binding to DEB has been shown to be fully reversible as the total dose can be extracted using a solution of potassium chloride and ethanol. Using improved elution models with open-loop flow through conditions as described by Swaine et al. may facilitate the modelling of full extended vandetanib release by preventing saturation of elution medium and more closely mimicking the *in vivo* situation (Swaine et al., 2016).

The addition of the iodinated moiety that renders DC Bead LUMI™ radiopaque increases the solid content of the beads (Duran et al., 2016) and introduces hydrophobic portions to the bead structure which may interact with various drugs thereby altering drug loading and release properties. Increasing loading of vandetanib also leads to a proportional increase in the radiopacity of the DC Bead LUMI™ (Fig. 4) which is not attributable to a densification of the internal structure as the mean diameter of the beads are essentially unchanged with drug loading (Fig. 2F). The existence of a bromine atom on the vandetanib structure is the likely source of the added radiopacity, which increases by approximately 25–26 Hounsfield units per mg of radiodense atom (iodine and bromine) present.

The data presented in this study has confirmed that DC Bead LUMI™ has desirable physicochemical characteristics suitable for use as an anti-angiogenic DEB. Firstly, maximum vandetanib loading capacity is high, reaching maximum doses of over 120 mg/mL at pH 6.8 and even when decreasing pH to maintain vandetanib solubility doses of 100 mg/mL are still feasible. The increased solid content leads to a higher density of drug binding sites than standard DC Bead™. This increased capacity may compensate for the slower drug release rate. Secondly, DC Bead LUMI™ was more resistant to size changes after loading with vandetanib, compared with DC Bead™ which had a significant reduction in bead size and volume. Although there has been a trend towards using smaller size beads in recent years (Lencioni et al., 2012), it has been observed that particles of around 40 μm pose a risk of potentially fatal complications resulting from off-target embolisation (Bonomo et al., 2010; Brown, 2004). The radiopacity of DC Bead LUMI ™ may also provide advantages in this respect due to the potential for intra and post-procedural feedback on bead delivery (Duran et al., 2016). Finally, loading of the drug did not adversely affect the properties of the beads in terms of their suspension, handling and delivery in contrast agent. When mixed into suspension only a small amount of drug (3.5 mg) was released into Omnipaque contrast agent and the drug was shown to be stable in this mixture over the 24 h storage condition selected for the test. These preliminary evaluations confirm that

vandetanib loaded DC Bead LUMI™ performs in a manner amenable for a DEB-TACE procedure.

Recent investigations have been performed using DC Bead™ loaded with the VEGFR inhibitor sunitinib (Fuchs et al., 2015; Fuchs et al., 2014), which have shown significant effects on endothelial cell proliferation, apoptosis and migration, with both sunitinib beads and free sunitinib having similar activity *in vitro*. Sunitinib beads had modest anti-proliferative effects against a range of cancer cell lines, with lack of direct cytotoxicity due to the mechanism of action of sunitinib being VEGFR inhibition. As well as inhibiting VEGFR, vandetanib also targets EGFR and therefore has the potential to also directly impede cancer cell proliferation and induce apoptosis. *In vitro* assays have revealed that vandetanib has a significant anti-proliferative effect on endothelial cells and induces apoptosis in hepatoma cell lines at a concentration of <10 μmol/L (4.75 μg/ml) (Inoue et al., 2012). The elution studies performed here indicate that the release of vandetanib levels in excess of this concentration is feasible. In support of this preliminary data we have recently reported on a safety and pharmacokinetics study of vandetanib DEB-TACE in healthy swine liver which demonstrated that the treatment was well tolerated and confirmed the presence of therapeutic concentrations of vandetanib up to 30 days after administration (Czuczman et al., 2016).

5. Conclusions

Vandetanib can be efficiently loaded and released from DC Bead™ and DC Bead LUMI™ whilst maintaining microsphere integrity and properties suitable for use as an embolization agent. The inclusion of vandetanib in a DEB warrants further characterisation *in vitro* and *in vivo* to determine its efficacy in models of HCC.

Acknowledgements

A. Hagan would like to thank the Royal Commission for the Exhibition of 1851 for provision of funding for an Industrial Fellowship.

References

Bize, P., et al., 2016. Antitumoral effect of sunitinib-eluting beads in the rabbit VX2 tumor model. Radiology 280 (2), 425–435.
Bonomo, G., et al., 2010. Bland embolization in patients with unresectable hepatocellular carcinoma using precise, tightly size-calibrated, anti-inflammatory microparticles: first clinical experience and one-year follow-up. Cardiovasc. Intervent. Radiol. 33 (3), 552–559.
Brown, K.T., 2004. Fatal pulmonary complications after arterial embolization with 40–120-micron tris-acryl gelatin microspheres. J. Vasc. Interv. Radiol. 15 (2 Pt 1), 197–200.
Bruix, J., Sala, M., Llovet, J.M., 2004. Chemoembolization for hepatocellular carcinoma. Gastroenterology 127 (5, Supplement 1), S179–S188.
Chao, M., et al., 2016. A nonrandomized cohort and a randomized study of local control of large hepatocarcinoma by targeting intratumoral lactic acidosis. Elife 5, e15691.
Chen, J., et al., 2014. Poly(lactide-*co*-glycolide) microspheres for MRI-monitored transcatheter delivery of sorafenib to liver tumors. J. Control. Release 184, 10–17.
Chen, J., et al., 2015. Poly(lactide-*co*-glycolide) microspheres for MRI-monitored delivery of sorafenib in a rabbit VX2 model. Biomaterials 61, 299–306.
Cheng, A.L., et al., 2013. Sunitinib versus sorafenib in advanced hepatocellular cancer: results of a randomized phase III trial. J. Clin. Oncol. 31 (32), 4067–4075.
Cox, J., Weinman, S., 2015. Mechanisms of doxorubicin resistance in hepatocellular carcinoma. Hepat. Oncol. 3 (1), 57–59.
Czuczman, P., et al., 2016. Elution of vandetanib from radiopaque drug-eluting beads in vitro and pharmacokinetics of vandetanib in swine following administration in radiopaque drug-eluting beads. CIRSE Annual Congress. Springer, Barcelona, Spain.
Duran, R., et al., 2016. A novel inherently radiopaque bead for transarterial embolization to treat liver cancer - a pre-clinical study. Theranostics 6 (1), 28–39.
Erhardt, A., et al., 2014. TACE plus sorafenib for the treatment of hepatocellular carcinoma: results of the multicenter, phase II SOCRATES trial. Cancer Chemother. Pharmacol. 74 (5), 947–954.
Forster, R.E., et al., 2010. Comparison of DC Bead-irinotecan and DC Bead-topotecan drug eluting beads for use in locoregional drug delivery to treat pancreatic cancer. J. Mater. Sci. Mater. Med. 21 (9), 2683–2690.
Forster, R.E., et al., 2012. Development of a combination drug-eluting bead: towards enhanced efficacy for locoregional tumour therapies. Anti-Cancer Drugs 23 (4), 355–369.
Fuchs, K., et al., 2014. Drug-eluting beads loaded with antiangiogenic agents for chemoembolization: in vitro sunitinib loading and release and in vivo pharmacokinetics in an animal model. J. Vasc. Interv. Radiol. 25 (3), 379–387.
Fuchs, K., et al., 2015. Sunitinib-eluting beads for chemoembolization: methods for in vitro evaluation of drug release. Int. J. Pharm. 482 (1–2), 68–74.
Gewirtz, D.A., 1999. A critical evaluation of the mechanisms of action proposed for the antitumor effects of the anthracycline antibiotics adriamycin and daunorubicin. Biochem. Pharmacol. 57 (7), 727–741.
Guiu, B., et al., 2015. Idarubicin-loaded ONCOZENE drug-eluting embolic agents for chemoembolization of hepatocellular carcinoma: in vitro loading and release and in vivo pharmacokinetics. J. Vasc. Interv. Radiol. 26 (2), 262–270.
Hecq, J.-D., et al., 2013. Doxorubicin-loaded drug-eluting beads (DC Bead®) for use in transarterial chemoembolization: a stability assessment. J. Oncol. Pharm. Pract. 19 (1), 65–74.
Hsu, C., et al., 2012. Vandetanib in patients with inoperable hepatocellular carcinoma: a phase II, randomized, double-blind, placebo-controlled study. J. Hepatol. 56 (5), 1097–1103.
Inoue, K., et al., 2012. Vandetanib, an inhibitor of VEGF receptor-2 and EGF receptor, suppresses tumor development and improves prognosis of liver cancer in mice. Clin. Cancer Res. 18 (14), 3924–3933.
Lahti, S.J., et al., 2015a. Sorafenib loaded drug-eluting beads: loading and eluting kinetics and in vitro viability study. J. Vasc. Interv. Radiol. 26 (2 (Suppl.)), S80–S81.
Lahti, S.J., et al., 2015b. Sunitinib loaded drug-eluting beads: loading and eluting kinetics and in vitro viability study. J. Vasc. Interv. Radiol. 26 (2 (Suppl.)), S81–S82.
Lencioni, R., et al., 2012. Transcatheter treatment of hepatocellular carcinoma with doxorubicin-loaded DC Bead (DEBDOX): technical recommendations. Cardiovasc. Intervent. Radiol. 35 (5), 980–985.
Lencioni, R., et al., 2016. Sorafenib or placebo plus TACE with doxorubicin-eluting beads for intermediate stage HCC: the SPACE trial. J. Hepatol. 64 (5), 1090–1098.
Levy, E.B., et al., 2016. First human experience with directly image-able iodinated embolization microbeads. Cardiovasc. Intervent. Radiol. 39 (8), 1177–1186.
Lewis, A.L., 2009. DC Bead™: a major development in the toolbox for the interventional oncologist. Expert Rev. Med. Devices 6 (4), 389–400.
Lewis, A.L., Dreher, M.R., 2012. Locoregional drug delivery using image-guided intra-arterial drug eluting bead therapy. J. Control. Release.
Lewis, A.L., Holden, R.R., 2011. DC Bead embolic drug-eluting bead: clinical application in the locoregional treatment of tumours. Expert Opin. Drug Deliv. 8 (2), 153–169.
Lewis, A.L., et al., 2007. Doxorubicin eluting beads - 1: effects of drug loading on bead characteristics and drug distribution. J. Mater. Sci. Mater. Med. 18 (9), 1691–1699.
Liang, B., et al., 2010. Correlation of hypoxia-inducible factor 1[alpha] with angiogenesis in liver tumors after transcatheter arterial embolization in an animal model. Cardiovasc. Intervent. Radiol. 33 (4), 806–812.
Morabito, A., et al., 2009. Vandetanib (ZD6474), a dual inhibitor of vascular endothelial growth factor receptor (VEGFR) and epidermal growth factor receptor (EGFR) tyrosine kinases: current status and future directions. Oncologist 14 (4), 378–390.
Namur, J., 2009. Microsphères d'embolisation Pour la Vectorisation de Principes Actifs: Étude de la Libération In Vivo par Microspectroscopies Optiques (Reims).
Park, W., et al., 2016. Acidic pH-triggered drug-eluting nanocomposites for magnetic resonance imaging-monitored intra-arterial drug delivery to hepatocellular carcinoma. ACS Appl. Mater. Interfaces 8 (20), 12711–12719.
Rhee, T.K., et al., 2007. Effect of transcatheter arterial embolization on levels of hypoxia-inducible factor-1α in rabbit VX2 liver tumors. J. Vasc. Interv. Radiol. 18 (5), 639–645.
Sakr, O.S., et al., 2016. Arming embolic beads with anti-VEGF antibodies and controlling their release using LbL technology. J. Control. Release 224, 199–207.
Sharma, K.V., et al., 2016. Long-term biocompatibility, imaging appearance and tissue effects associated with delivery of a novel radiopaque embolization bead for image-guided therapy. Biomaterials 103, 293–304.
Swaine, T., et al., 2016. Evaluation of ion exchange processes in drug-eluting embolization beads by use of an improved flow-through elution method. Eur. J. Pharm. Sci. 93, 351–359.
Taylor, R.R., et al., 2007. Irinotecan drug eluting beads for use in chemoembolization: in vitro and in vivo evaluation of drug release properties. Eur. J. Pharm. Sci. 30 (1), 7–14.
Tsang, V.H., Robinson, B.G., Learoyd, D.L., 2016. The safety of vandetanib for the treatment of thyroid cancer. Expert Opin. Drug Saf. 15 (8), 1107–1113.
Wang, Y., et al., 2015. Preparation and structure of drug-carrying biodegradable microspheres designed for transarterial chemoembolization therapy. J. Biomater. Sci. Polym. Ed. 26 (2), 77–91.
Wang, Y., et al., 2016. In vitro and in vivo evaluation of drug-eluting microspheres designed for transarterial chemoembolization therapy. Int. J. Pharm. 503 (1–2), 150–162.